Published in final edited form as:
J Mater Chem B Mater Biol Med. 2014 November 7; 2(41): 7109–7113. doi:10.1039/C4TB01094A.

ROS-cleavable proline oligomer crosslinking of polycaprolactone for pro-angiogenic host response

Sue Hyun Lee[a], **Timothy C. Boire**[a], **Jung Bok Lee**[a], **Mukesh K. Gupta**[a], **Angela L. Zachman**[a], **Rutwik Rath**[a], and **Hak-Joon Sung**[a]

Hak-Joon Sung: hak-joon.sung@vanderbilt.edu

[a]Department of Biomedical Engineering, Vanderbilt University, Nashville TN 37235, USA. Tel: +1-6153226986

Abstract

A reactive oxygen species (ROS)-degradable scaffold is fabricated by crosslinking biocompatible, hydrolytically-degradable poly(ε-caprolactone) (PCL) with a ROS-degradable oligoproline peptide, KP_7K. The ROS-mediated degradability triggers favorable host responses of the scaffold including improved cell infiltration and angiogenesis *in vivo*, indicating its unique advantages for tissue engineering applications.

Recent progress in biomaterial development emphasizes the advanced function that enables target-specific therapeutic delivery through a stimuli-responsive structural change in a spatiotemporally controlled manner. These materials have been designed to activate the advanced functions in response to various physiological parameters, such as pH,[2] temperature,[3] protease activities, and redox balance[4]to target a local pathological event in the body. One such biological stimulus that is drawing keen attention recently is reactive oxygen species (ROS) which include hydroxyl radicals(OH.), hydrogen peroxides(H_2O_2), peroxynitrites($ONOO^-$) and superoxides(O_2^-) among others.[5]While low levels of ROS are part of normal cell metabolism, excessive amounts of ROS cause oxidative stress and damage critical components of cells at all levels including DNA, [6] proteins,[7] and lipids[8] by oxidation. Moreover, chronically increased levels of ROS are present locally in cancer,[9] atherosclerosis,[10] diabetes,[11] infections,[12] inflammatory diseases,[13] and even in the aging process[14] where ROS levels can be 10- to 100-times the normal levels. For example, in the vicinity of activated macrophages that are prevalent in inflammation and implantation sites, the hydrogen peroxide concentration can reach 10 – 100 μM.[15] Therefore, ROS can be considered as a critical parameter indicating local occurrence or progression of such diseases, and ROS-responsive materials are needed to enable site-specific delivery of therapeutics and imaging agents as they can undergo structural changes (e.g., degradation) and release the payload in response to locally overproduced ROS *in vivo*.

Correspondence to: Hak-Joon Sung, hak-joon.sung@vanderbilt.edu.

†Electronic Supplementary Information (ESI) available: 1H-NMR and characterization of bone marrow-derived macrophages used in *in vitro* experiments. See DOI: 10.1039/c000000x/

Starting with polypropylene sulfide (PPS) developed in 2004, ROS-sensitive materials are still relatively new, but have been continuously developed due to the increasing demand for various biomedical applications. While numerous other studies focused on designing synthetic polymers that rapidly respond to ROS in nanoscale delivery formats [16,17,18], we investigated a peptide oligomerasa ROS-responsive unitfor long-term tissue engineering applications. Previous studies have shown that proteins containing aspartic acid, glutamic acid orproline residues are especially prone to oxidative degradation. [19] ROS-sensitive degradability of proline residues has demonstrated particular promise.[20, 21]

In a previous study, we synthesized proline oligomers as a ROS-cleavable crosslinker and extensively characterized its fabrication and response to ROS *in vitro*.[22] In particular, oligoproline peptides with 5 or 7 or 10 proline residues were tested for ROS-mediated degradation by reactingin 5 mM H_2O_2 with 50 μMCu(II) at 37°C. All proline residues were cleaved away after 6 days, confirming relatively slow ROS-mediated degradation, compared to PPS that degrades in several hours under oxidative environment.[16]

Therefore, in the current study, we investigated the potential of using an oligoproline-crosslinked poly(ε-caprolactone) (PCL)-based scaffold in an *in vivo* model for long-term tissue engineering applications. PCL was chosen as the base polymer,as it is approved by the Food and Drug Administration (FDA) for biomedical applications such as tissue engineering and drug delivery.[23] Furthermore, PCL is known for slow *in vivo* degradation over several years by hydrolysis of ester bonds, thereby providing a material format where we can impart faster-acting ROS-degradability to the scaffold. We hypothesized that such ROS-degradability of scaffolds would allow for favourable interactions with host cells *in vivo* where the initial inflammatory host response would degrade the implanted scaffold by excess ROS production and encourage cell infiltration into the scaffold, leading to improved neovascularization and engraftment within the site of implantation.[24] Towards this end, first we modified and improved the chemistry involved to efficiently crosslink PCL with ROS-degradable oligoproline peptides, and studied their chemical and thermal properties as well as their *in vitro* ROS-degradability. Finally, we implanted the scaffolds subcutaneously in mice to test our hypothesis for the effect of ROS-degradability of scaffold on host-material interaction with an emphasis on vascularization of the implanted scaffold.

To incorporate crosslinkers, PCL was functionalized with carboxyl groups (Fig. 1A).[25] The ratio of the integral peaks for carboxylated PCL (CPCL) (3.4 and 9.2 ppm) and unmodified PCL (4.1 ppm) from the ^{1}H-NMR spectrum revealed a molar composition of 70%PCL-30% CPCL (Fig. S1). Of note, the extent of carboxylation can be varied from 5 - 60% by varying the duration of the reaction (data not shown).The molecular weight of 70% PCL-30% CPCL (number-average molecular weight (M_n) = 95.5 kDa; polydispersity (PDI = M_w/M_n) of 1.40) is comparable to the unmodified starting material, 100%PCL (M_n = 87.0 kDa; PDI = 1.28), indicating no significant hydrolysis of polyester chains during the reaction with LDA. Fig. 1B shows the ROS-cleavable KP_7K peptide crosslinker and poly(ethylene glycol) (PEG)-dihydrazide crosslinker used as a control in this study. Dicyclohexylcarbodiimide (DCC)/N-hydroxy-succinimide ester (NHS) was used to crosslink 70% PCL-30% CPCL with the crosslinkers. Rapid crosslinking was observed asthe mixture began gelling immediately.

We then verified and characterized the crosslinking. Successful crosslinking was first confirmed by FTIR, where amide (I) C=O band at ~1620 cm^{-1} was observed for both PEG-dihydrazide and KP_7K-crosslinked 70% PCL-30% CPCL, as well as increased absorbance for N-H stretching and O-H stretching from water molecules around 3200~3700 cm^{-1} (Fig. 2A).[26] Next, gel content measurement further characterized the degree of crosslinking, where PEG-dihydrazide and KP_7K-crosslinked scaffolds exhibited 73±7.1% and 82±5.9% in gel contents with THF washes, respectively, indicating a high degree of crosslinking within these scaffolds.

Crosslinking of 70% PCL-30% CPCL with hydrophilic KP_7K peptide crosslinkers altered physicochemical properties of the scaffolds, as evidenced by the changes in the swelling ratios of the scaffolds. When incubated in PBS at 37 °C for 1 day, uncrosslinked 30% CPCL-70% PCL had significantly increased the swelling ratio compared to original PCL, and the highly hydrophilic nature of both crosslinkers further increased the swelling ratios of the crosslinked scaffolds (Fig. 2B). Such increases in hydrophilicity are desirable as it may improve cell attachment and infiltration compared to hydrophobic 100% PCL *in vivo*. [27]

Similarly, the series of modifications made on PCL significantly altered the thermal properties (Fig. 2C). First, carboxylation of PCL resulted in reduced heats of crystallization (ΔH_c) and melting (ΔH_f), as the carboxyl groups disrupted the packing of semi-crystalline PCL chains to some degree and resulted in less crystallinity. Then, the crosslinking of KP_7K or PEG-dihydrzide with 70% PCL-30% CPCL further disrupted the crystallinity of PCL and reduced the polymer chain flexibility, resulting in drastic decreases in temperatures of crystallization (T_c) and melting (T_m), as well as in ΔH_c and ΔH_f.[28] These changes in the thermal properties resulting from carboxylation and crosslinking can significantly influence material properties, which was exhibited in elastic modulus measured by dynamic mechanical analysis (DMA). Non-porous, thin films were prepared and measured for their elastic moduli in wet conditions at 37 °C. While PCL and 70% PCL-30% CPCL were similar at 77.0 ± 6.0 MPa and 82.5 ± 4.7 MPa, respectively, both PEG- and KP7K-crosslinked conditions exhibited significantly reduced elastic moduli at 22.7 ± 2.7 MPa and 46.4 ± 0.4 MPa (each condition with N=3). The drastic decreases in elastic moduli in the crosslinked conditions are likely due to the decreases in crystallinity (T_c and ΔH_c), caused by crosslinking. Thus, we have shown and proven the effects of crosslinking on PCL in several aspects.

The ROS-degradability of KP_7K-crosslinked scaffold was demonstrated by changes in thermal properties (Fig. 3A). Scaffolds were incubated in PBS at 37 °C with or without daily changes of 1 mM SIN-1 for 30 days which degrades into superoxides and nitric oxides to form peroxynitrites.[29] Most notably,the T_c value of the KP_7K-crosslinked scaffold increased significantly with SIN-1 treatment compared to the ones of day 0 and PBS only condition on day 30, as radicals produced from SIN-1 degraded KP_7K crosslinkers, and the newly freed polymer chains likely underwent reorganization and recrystallization.[28] In contrast,the uncrosslinked PCL and 70%PCL-30% CPCL scaffolds showed minimal changes in the T_c. PEG-crosslinked scaffolds also degraded with SIN-1 treatment, albeit to a lesser degree than the KP_7K-crosslinked scaffolds. Interestingly, Reid et al. has shown that PEG also degrades in response to ROS produced from Fenton reaction with 50% (w/v) H_2O_2 and 6.2 mM $FeCl_3$

or from radicals produced by UV degradation of 30% H_2O_2.[30] However, PEG and PEG-crosslinked scaffolds might require supraphysiological levels of ROS for degradation which may not be biologically relevant.

The degradation of KP_7K scaffold was accelerated in a physiologically relevant ROS environment *in vitro* where mouse bone marrow-derived macrophages (BMDMs, see the cell characterization in Fig. S2A) were seeded on the scaffolds with or without the stimulation with 50 μg/ml LPS (Fig. 3B-C).[31] As an endotoxin, LPS activates macrophages to overproduce ROS and reactive nitrogen species (RNS) including nitric oxide (NO•), nitrite(NO_2^-) and peroxynitrite ($ONOO^-$) (Fig. S2B).[32] After removing cells and protein debris from the scaffold, the scaffold surface was imaged by scanning electron microscopy (SEM) (Fig. 3B). ROS-cleavable KP_7K-crosslinked scaffolds evidently formed numerous pores < 1 μm^2, especially when seeded with LPS activated BMDMs, while PEG-crosslinked scaffolds appeared to maintain their smooth surface over 7 day culture. Quantification of this pore formation after 7 day culture (Fig. 3C) reveals that sub-micron diameter pores increased by more than 10-folds for KP_7K-crosslinked scaffolds cultured with LPS-activated BMDMs, whereas when cultured without LPS, the pore generation was minimal. These results prove that KP_7K-crosslinked scaffolds degrade in response to the physiological levels of ROS produced by activated BMDMs.

PCL is known to slowly undergo hydrolytic chain scission over several years and become 6-hydroxylcaproic acids that are safely removed from the body.[33] We expected that the initial host immune response to implants would degrade ROS-degradable KP_7K into α-aminobutyric acids that can be used for biosynthesis, while leaving PEG crosslinkers intact due to its non-biodegradability.[34] Therefore, we tested our hypothesis that ROS-degradability of the scaffolds would encourage cell infiltration in a host-responsive manner, thereby improving vascularization of the constructs *in vivo* (Fig. 4). Scaffolds were subcutaneously implanted in mice for 2 weeks, and sections were stained with H&E to determine host cell infiltration (Fig. 4A). While cell infiltration is observed in all the test groups, there are some noticeable differences between the materials. When the density of nuclei ismeasured per tissue/scaffold area from H&E stained sections (Fig. 4B), it is evident that PCL-30% CPCL had significantly less cells infiltrating compared to PCL, possibly due to the negative charges on carboxyl groups with degreased protein adsorption. PEG-crosslinked scaffolds showed a similar number of infiltrating host cells compared to PCL. More importantly, KP_7K-crosslinked scaffolds exhibited the highest nuclei density with 50% more cells infiltrating compared to PCL. Additionally, mice were perfused through the heart with fluorescent microbeads for angiography before harvesting[35] (Fig. 4A), and the implanted scaffolds were collected for gene expression analysis (Fig. 4C). While PCL-30% CPCL and PEG-crosslinked scaffolds showed similarly higher levels of neovasculature formation compared to PCL, KP_7K-crosslinked scaffolds significantly promoted angiogenesis, as evidenced by abundant functional, perfusable blood vessels shown in the angiograms, compared to those of PCL scaffolds. This result was further supported by significant increases in gene expression of angiogenesis markers (CD31 and VEGFA)[36]assessed by quantitative RT-PCR (Fig. 4C), indicating that crosslinking with KP_7K significantly increases blood vessel growth into the scaffolds upon implantation. This

is likely due to the fact that early inflammatory responses resulted in degradation of KP_7K-crosslinked scaffolds, which enhances cell infiltration and growth of host cells into the implanted scaffolds, thereby promoting angiogenesis, compared to other conditions that degrade slowly through hydrolysis only. It is also possible that the oligoproline peptides themselves may have collagen-mimetic functions and properties, as oligoproline peptides mimic collagen in both chemical composition and structure[37]. However, further studies are required to confirm this possibility.

Conclusions

This study demonstrated synthesis and crosslinking of 70% PCL-30% CPCL with ROS-cleavable KP_7K and PEG-dihydrazide crosslinkers via DCC/NHS coupling. To examine their ROS-mediated degradation in a physiologically relevant condition, BMDMs were cultured on the scaffolds under LPS treatment to stimulate their ROS overproduction *in vitro*. The KP_7K-crosslinked scaffolds underwent significant surface degradation in response to overproduced ROS from activated BMDMs. Furthermore, angiogenesis was significantly promoted within the implanted KP_7K-crosslinked scaffolds. This pro-angiogenic behavior can likely be explained by ROS production from host inflammatory cells which induce scaffold degradation and pore generation, resulting in enhanced host cell infiltration into the scaffolds. We have shown that KP_7K-crosslinked 70%PCL-30%CPCL is 1) degradable in response to physiologically relevant ROS levels which allows for better host cell infiltration, and 2) pro-angiogenic *in vivo* via host-material interactions.

While various stimuli-sensitive materials have been developed innano- to microscale formats as drug delivery vehicles, applying large-scale stimuli-sensitive scaffolds for tissue engineering remain underexplored. Here, we demonstrated the unique advantages of applying ROS-responsive scaffolds in improving vascularization, which is currently an unmet need in the field of tissue engineering. Further studies are required to understand the mechanism by which ROS-degradable KP_7K-crosslinked scaffolds promote angiogenesis with favorable host response. In this way, the scaffold design can be improved to achieve successful engraftment and better clinical outcomes in the future.

Supplementary Material

Refer to Web version on PubMed Central for supplementary material.

Acknowledgments

This study was supported by NSF CAREER CBET 1056046. This study employed the use of resources at the Vanderbilt Institute of Nanoscale Science and Engineering (VINSE), a facility renovated under NSF ARI-R2 DMR-0963361. Confocal microscopy was performed through the use of the VUMC Cell Imaging Shared Resource (supported by NIH grants CA68485, DK20593, DK58404, HD15052, DK59637 and EY08126). ^{1}H-NMR was conducted in the Vanderbilt Small Molecule NMR Facility Core.

References

1. Yu SS, Koblin RL, Zachman AL, Perrien DS, Hofmeister LH, Giorgio TD, Sung HJ. Biomacromolecules. 2011; 12:4357–4366. [PubMed: 22017359]
2. Schoener CA, Hutson HN, Peppas NA. Polym Int. 2012; 61:874–879. [PubMed: 23087546]

3. Cammas S, Suzuki K, Sone C, Sakurai Y, Kataoka K, Okano T. Journal of Controlled Release. 1997; 48:157–164.
4. Meng F, Zhong Z, Feijen J. Biomacromolecules. 2009; 10:197–209. [PubMed: 19123775]
5. Papa S, Skulachev VP. Molecular and cellular biochemistry. 1997; 174:305–319. [PubMed: 9309704]
6. Wiseman H, Halliwell B. Journal of biochemistry. 1996; 313:17–29.
7. Dean RT, Fu S, Stocker R, Davies MJ. The Biochemical journal. 1997; 324(Pt 1):1–18. [PubMed: 9164834]
8. Aitken RJ, Clarkson JS, Fishel S. Biology of reproduction. 1989; 41:183–197. [PubMed: 2553141]
9. Vaccari L, Canton D, Zaffaroni N, Villa R, Tormen M, di Fabrizio E. Microelectronic Engineering. 2006; 83:1598–1601.
10. Sugamura K, Keaney JF. Free Radical Biology & Medicine. 2011; 51:978–992. [PubMed: 21627987]
11. Houstis N, Rosen ED, Lander ES. Nature. 2006; 440:944–948. [PubMed: 16612386]
12. Rastew E, Vicente JB, Singh U. Int J Parasitol. 2012; 42:1007–1015. [PubMed: 23009748]
13. Rahman I. J Biochem Mol Biol. 2003; 36:95–109. [PubMed: 12542980]
14. Papp LV, Lu J, Holmgren A, Khanna KK. Antioxidants & redox signaling. 2007; 9:775–806. [PubMed: 17508906]
15. Droge W. Physiol Rev. 2002; 82:47–95. [PubMed: 11773609]
16. Napoli A, Valentini M, Tirelli N, Muller M, Hubbell JA. Nature materials. 2004; 3:183–189.
17. Wilson D, Dalmasso G, Wang L, Sitaraman S, Merlin D, Murthy N. Nautre Materials. 2010; 9:923–928.
18. Lee SH, Gupta MK, Bang JB, Bae H, Sung HJ. Advanced Healthcare Materials. 2013; 2:908–915. [PubMed: 25136729]
19. Stadtman ER, Levine RL. Amino acids. 2003; 25:207–218. [PubMed: 14661084]
20. Garrison WM. Chem Rev. 1987; 87:381–398.
21. Amici, a; Levine, RL.; Tsai, L.; Stadtman, ER. The Journal of biological chemistry. 1989; 264:3341–3346. [PubMed: 2563380]
22. Yu SS, Koblin RL, Zachman AL, Perrien DS, Hofmeister LH, Giorgio TD, Sung HJ. Biomacromolecules. 2011; 12:4357–4366. [PubMed: 22017359]
23. Lam CX, Hutmacher DW, Schantz JT, Woodruff MA, Teoh SH. Journal of biomedical materials research Part A. 2009; 90:906–919. [PubMed: 18646204]
24. Sung HJ, Meredith C, Johnson C, Galis ZS. Biomaterials. 2004; 25:5735–5742. [PubMed: 15147819]
25. Gupta MK, Walthall JM, Venkataraman R, Crowder SW, Jung DK, Yu SS, Feaster TK, Wang X, Giorgio TD, Hong CC, Baudenbacher FJ, Hatzopoulos AK, Sung HJ. PloS one. 2011; 6:e28935. [PubMed: 22216144]
26. Movasaghi Z, Rehman S, Rehman DIur. Applied Spectroscopy Reviews. 2008; 43:134–179.
27. Ma Z, Mao Z, Gao C. Colloids and surfaces B, Biointerfaces. 2007; 60:137–157.
28. Mandelkern L. Chem Rev. 1995; 56:903–958.
29. Hogg N, Darley-Usmar V, WIlson M, Mocada S. Biochem J. 1992; 281:419–424. [PubMed: 1310595]
30. Reid B, Gibson M, Singh A, Taube J, Furlong C, Murcia M, Elisseeff J. Journal of tissue engineering and regenerative medicine. 201310.1002/term.1688
31. Weischenfeldt J, Porse B. CSH protocols. 2008 2008, pdb prot5080.
32. Amatore C, Arbault S, Bouton C, Drapier JC, Ghandour H, Koh AC. Chembiochem : a European journal of chemical biology. 2008; 9:1472–1480. [PubMed: 18491327]
33. Woodruff MA, Hutmacher DW. Progress in Polymer Science. 2010; 35:1217–1256.
34. Knop K, Hoogenboom R, Fischer D, Schubertf US. Angew Chem Int Ed. 2010; 49:6288–6308.
35. Zachman AL, Crowder SW, Ortiz O, Zienkiewicz KJ, Bronikowski CM, Yu SS, Giorgio TD, Guelcher SA, Kohn J, Sung HJ. Tissue engineering Part A. 2013; 19:437–447. [PubMed: 22953721]

36. Mineo TC. Journal of Clinical Pathology. 2004; 57:591–597. [PubMed: 15166262]
37. Gorgieva S, Kokol V. 2 Collagen- vs Gelatin. 2011 inTech.

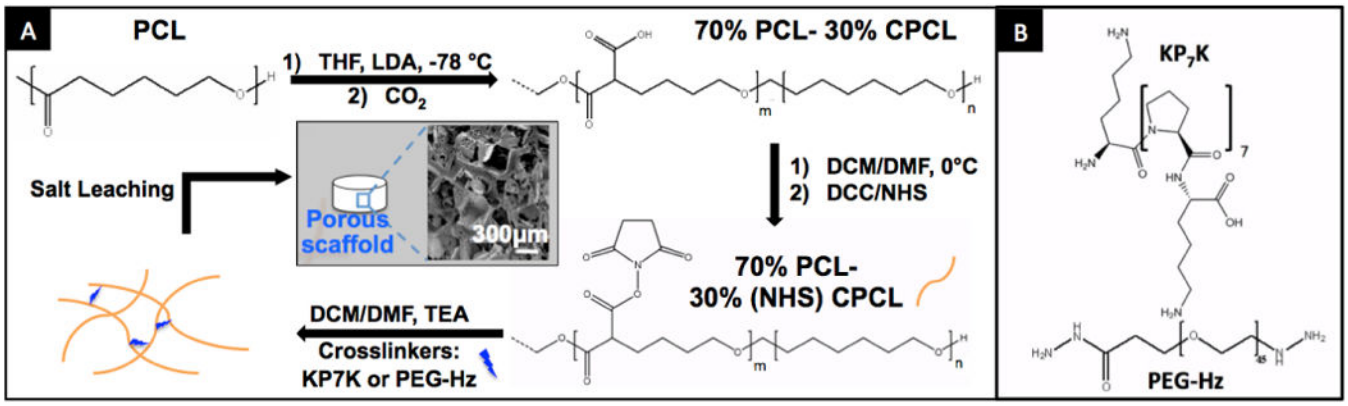

Fig. 1.

(A) Synthesis and fabrication of porous KP_7K or PEG-crosslinked 70%PCL-30%CPCL scaffolds with a representative SEM image. **(B)** ROS-cleavable peptide KP_7K[1] and PEG-dihydrazide (control) crosslinkers.

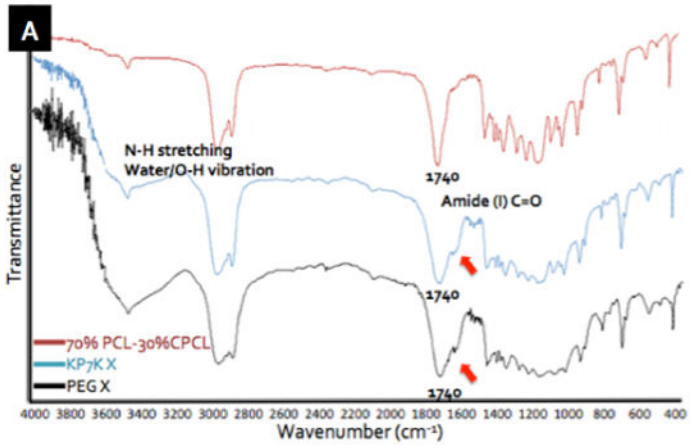

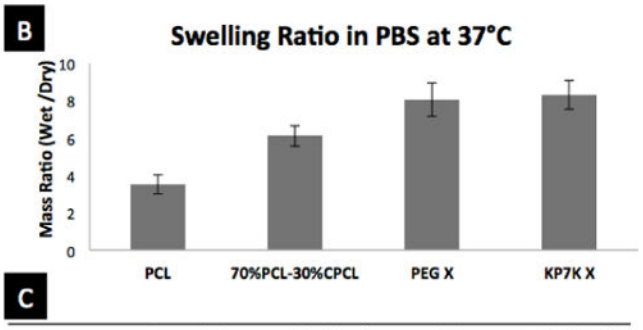

C

	Tc (C°)	ΔHc (J*g-1*C°-1)	Tm (C°)	ΔHf (J*g-1*C°-1)
PCL	28.9	73.1	55.1	71.7
70%PCL-30%CPCL	29.7	60.1	55.3	52.5
PEG X	10.2	37.4	43.1	33.9
KP7K X	14.0	34.6	42.5	33.0

Fig. 2.

Characterization of scaffolds. **(A)** FTIR spec for 70%PCL-30%CPCL crosslinked with either KP_7K (KP_7K X) or PEG-Hz (PEG X). (B) Swelling ratios of porous scaffolds. Error bar= ±1 SD. **(C)** Thermal characterization of porous scaffolds byDSC.

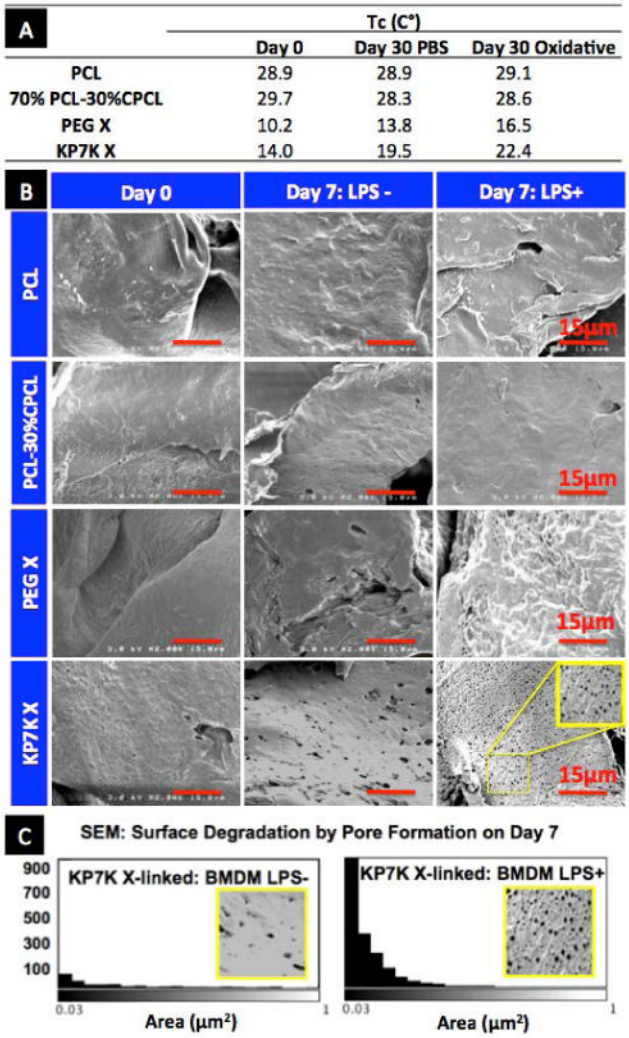

Fig. 3.

Characterization of scaffold degradation in response to ROS *in vitro*. **(A)** T_c values of scaffolds obtained from DSC after daily changes of PBS with or without 1mM SIN-1 over 30 days at 37°C. **(B)** SEM images of the scaffold surface after culturing mousebone marrow-derived macrophages (BMDMs)for 7 days with or without LPS stimulation. **(C)** Quantification of pores created by BMDMs on KP_7K-crosslinked scaffold surface on day 7.

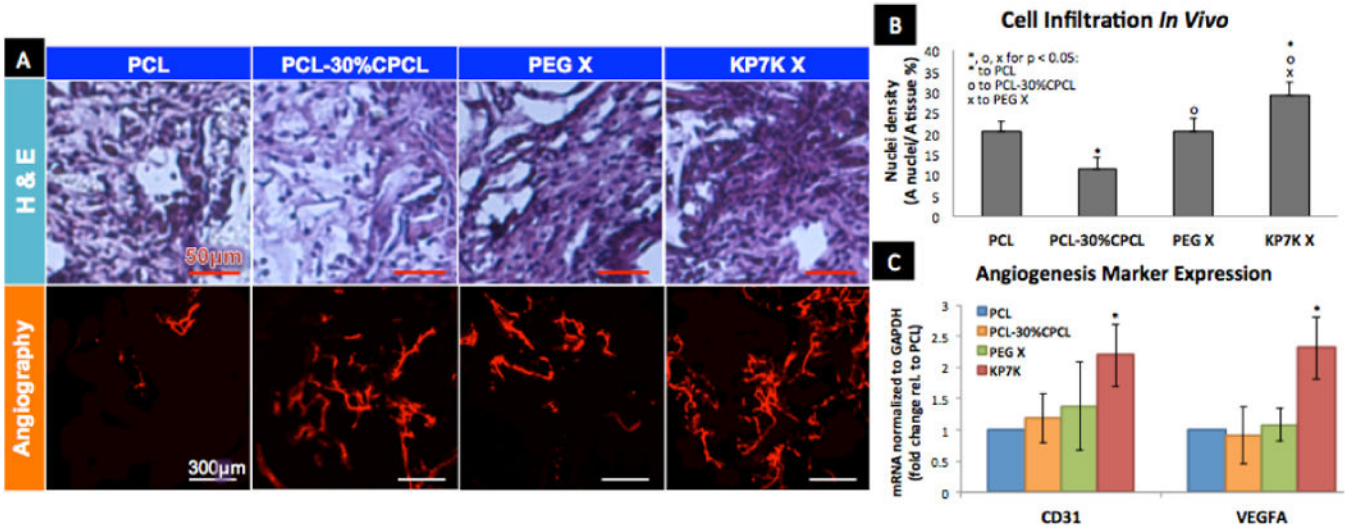

Fig. 4.

(A) After 2-week subcutaneous implantation, scaffolds were stained with H&E (purple: cytoplasm, dark blue: nuclei; scale bar = 50 μm), and imaged for angiography (scale bar = 300 μm). **(B)** Cell infiltration was quantified by Area (nuclei) / Area (tissue) (%) from H&E stained sections. **(C)** mRNA expression of angiogenesis markers by qRT-PCR (N=4; Error = ±1 SEM).